

*From the Research Laboratories
В изследователските лаборатории*

OBSERVING CHANGE IN POTASSIUM ABUNDANCE IN A SOIL EROSION EXPERIMENT WITH FIELD INFRARED SPECTROSCOPY

**Mila Ivanova Luleva, Harald van der Werff,
Freek van der Meer, Victor Jetten**
University of Twente, The Netherlands

Abstract. Soil erosion has been studied extensively in the last decades. Studies on soil particle movement through chemical tracers were mostly based on the use of radioactive elements. These however have a limited half-life, and are highly toxic and expensive to measure over large areas. This study examines the possibility to use Potassium (K), in the form of an agricultural fertilizer, as a soil particle tracer. Soluble Potassium is spectrally active and has an absorption feature near 2465 nm. This research hypothesises that flowing water moves surface soil particles with adsorbed K and can be traced by observing the change in absorption feature. A field-based water flow experiment was conducted on 3 plots in silty loam soils in the Netherlands. Two plots were treated with 0.6 and 2.48 mg/g of K₂O fertilizer, and one plot was used as reference. Infrared reflectance spectra were collected to observe spatial variation in available K, before and after application of fertilizer, and after runoff simulation by water flow. Change in absorption feature depth near 2465nm was used to determine K abundance, and maps with K distribution were produced for each stage of the experiment. Laboratory analysis was done to validate and explain the field results. Statistical relationships between absorption feature parameters of K, water and clay were established to determine whether K was removed during the experiment. Based on coefficients of determination (R^2), it can be concluded that an increase in moisture and clay content in a soil of over 18% poses a practical limitation in the use of K as a soil particle tracer with field infrared spectroscopy.

Keywords: potassium, SWIR, ASD spectroscopy, soil erosion

Introduction

Soil erosion and sedimentation have been studied extensively in the last decades (Boardman, 2006). An approach to predict soil erosion is to use chemical tracers (Onda et al., 2007) as a proxy for tracking of eroding soil particles (Zhang et al., 2001). Soil particles are moved by wind, water or gravity (Morgan, 2005). Soil particle tracing is an approach to measure net soil flux in arid and semi-arid environments and to detect early signs of hazard (Chappell, 1999). The cesium 137 isotope (¹³⁷Cs) is considered to

be the primary chemical tracer for detection of soil particle movement. This element has been used in a number of soil erosion studies for over 40 years. Most recent papers cover the use of ^{137}Cs either for comparison between various methods (Saç et al., 2008; Xiaojun et al., 2010), or as a validation technique of historical records (deGraffenried, Jr & Shepherd, 2009; Estrany et al., 2010; Meusburger et al., 2010; Rodway-Dyer & Walling, 2010). ^{137}Cs was introduced to the environment between the 1950s and 1970s through nuclear fallout of atomic bomb tests, and in 1986 through the Chernobyl power plant accident. Once fallen onto the Earth surface, ^{137}Cs attaches to soil particles. Its redistribution is mainly controlled by erosion, transport and deposition of sediments (Porto et al., 2001). The use of ^{137}Cs for soil particle tracking has some assumptions (Parsons & Foster, 2011): the distribution of ^{137}Cs fall out is homogeneous (while being limited to the Northern hemisphere), and particles would only move by the influence of soil erosion (Campbell et al., 1982; Chappell, 1999; Walling & Quine, 1990). Furthermore, the use is limited by the half-life of the isotope and the cost of soil chemical analysis, preventing its use over large areas (Boardman, 2006). There is hence a demand for a substitute of ^{137}Cs by a chemical element that has similar physical and chemical behaviour, can be distributed evenly in the environment and can be measured with already established analytical techniques.

Remote sensing allows the acquisition of continuous spatial information over larger areas (Alatorre & Beguería, 2009; Jetten et al., 2003; Vrieling, 2006). Recently, we suggested in Luleva et al. (2011) that the spectrally active element potassium (K) can be used as a proxy to ^{137}Cs in soil particle tracing. Potassium (K) has similar electrical, chemical and physical properties to Cs (Andrello & Appoloni, 2004; Relman, 1956), and both elements show similar chemical behaviour in the environment. A spectral absorption feature near 2465 nm is indicative for the abundance of K in soils, and absorption band depth is linearly related to concentration (Luleva et al., 2011).

Potassium (K) is found in soils in three forms: readily available to plants in a water soluble form, slowly available when released from clay minerals and unavailable as part of the crystalline structure of soil minerals. Potassium (K) can be introduced as a fertilizer in the form of potassium oxide (K_2O). The recommended amount of fertilizer for EU countries is 0.6-2 mg/g of soil, although quantities may be higher.¹⁾ When applied as a fertilizer, the majority of available K ions adsorb onto the surface of soil particles in the first 30 seconds to 2 minutes after application. When soils are not plowed, 1.003 mg of K per gram of soil is adsorbed, while if soils are disturbed, this amount reduces depending on quantity of removed organic matter in soil (Wang & Huang, 2001). The mobility of K is determined by various factors, the most important of which include physical and chemical properties such as texture (Luleva et al., 2011), organic matter (Askegaard & Eriksen, 2000); cation exchange capacity and presence of calcium, so-

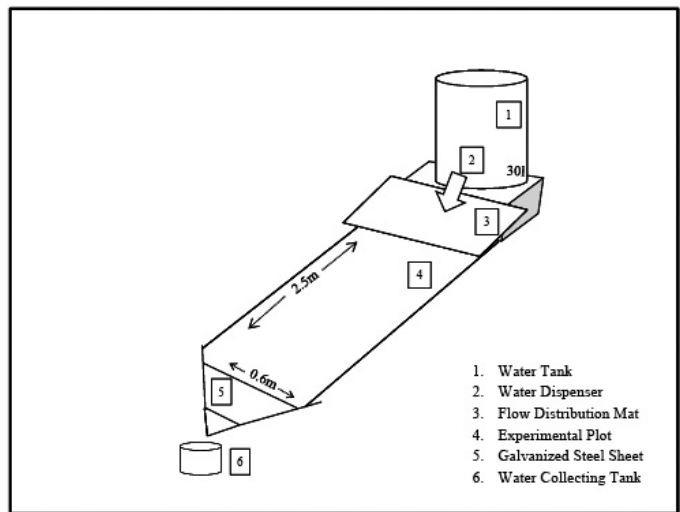
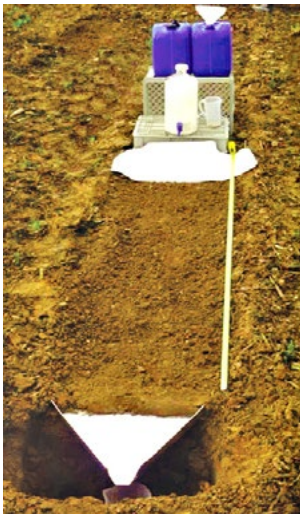
dium and gypsum (Jalali & Rowell, 2003; 2009). The aim of this study is to determine whether change in K concentration, when applied in the form of commercially available K fertilizer in concentrations commonly applied in agriculture, can be observed using field infrared spectroscopy.

We will examine this by answering three questions: (i) can a relative change in abundance of K in the field be observed with spectroscopy using the absorption feature near 2465 nm; (ii) does the amount of K removed by water flow correspond to the concentration of K found in runoff water; (iii) does a change in depth of the 2465nm absorption feature correspond with the controlled addition and removal of K.

Methods

Field experiment design

A standard practice in soil erosion studies is the use of experimental plots (Morgan, 2005). In this research, we did a field-based experiment with three experimental plots. Each plot was sprayed with a different concentration of K fertilizer. Controlled water flow generated soil erosion and runoff. The three plots were 2.5 m in length and 0.6 m in width, following Morgan (2005). Each plot was evened out and cleared from larger soil aggregates or loose vegetation residuals to achieve optimal flow conditions. Plot



a)

b)

Fig. 1. Experimental plot set up and components: a) photo of the setup in the field, “available in color online”; b) a schematic diagram of the setup

edges were raised 5-10cm above the soil surface to contain the runoff. The degree of slope naturally varied from 9.0% to 9.6%. Thirty litre water tanks with dispenser were used to generate water flow and doormats to distribute the flow evenly. Galvanized steel sheets placed at the bottom of each plot (20 cm below the surface) were used to collect runoff into collector tanks (Fig. 1).

400 ml of commercially available K fertilizer (K_2O) solution was sprayed onto each plot, one with 0.6mg/g (plot A) and one with 2.48 mg/g concentration (plot B). Plot C was used as a reference to observe the behaviour of naturally occurring K under the influence of flowing water. The duration of the flow was 14 - 20 min., depending on the path of the flow. 10l of runoff water and eroded soil were collected at the bottom of the plot during the flow simulation, which corresponds with a rainfall event of 90 mm per hour.

Field data collection

Before and after the flow experiment, silty loam soil samples for validation were collected from the surface (0-2cm) and at 15cm depth of each plot, following a grid-point sampling strategy (Hengl et al., 2003). Initial moisture content was measured in the field using an IRROMETER Watermark soil moisture meter. Water samples were collected per litre of runoff water, up to a maximum of 10 samples or until runoff had stopped. Additional mixed water samples were collected from the runoff tank in addition, taken from the surface, 10cm and 20cm depth.

Infrared spectral measurements were acquired with an Analytical Spectral Devices (ASD) Fieldspec Pro instrument with a 450 – 2500 nm wavelength range coverage at a 2-3 nm spectral resolution. The fore-optic was a high-intensity contact probe with internal light source and a spot size of 10 mm in diameter. The measurements were collected in three stages: prior to application of fertilizer to determine background values of K, after application of fertilizer to establish the distribution of fertilizer, and after water flow to observe particle displacement. Data were obtained in a grid with 6 measurements across flow direction and 18 measurements along flow direction, up to a total of 108 measurements per plot per stage. The same locations were measured at each stage of the experiment.

Geochemical analysis

The soil samples were dried overnight at 30° Celsius and sieved through a 2mm sieve to remove large particles. Water samples were filtered using laboratory membrane filters and the residual sediments were air dried overnight. All samples were analysed for total K content following standard laboratory procedures²⁾ with Inductively Coupled Plasma-Optical Emission Spectroscopy (ICP-OES) to a detection limit of 0.01 mg/ml. Texture and bulk density analyses were performed to determine the sand-silt-clay fractions.

The relationship between water contents and spectral absorption of K was analysed in a laboratory. A soil sample was passed through a 2 mm sieve and evenly distributed in three sample dishes, each dish containing approximately 50 grams of dry material. Three different concentrations of K fertilizer were added. The first set as a reference with addition of 10 ml of demineralized water and 0 mg/g of K, the remaining two with addition of 1.20 mg K/ g of soil and 2.48 mg K/g of soil in 10 ml solution respectively.

Spectral absorption was measured under laboratory conditions using the same instrument specifications and settings as during the field experiment. Collection of spectra was done for 6 contiguous hours over 2 days, adding up to a total of 117 measurements. Each sample was weighed before spectra were collected in order to measure the amount of moisture that had evaporated. The experiment was terminated when the initial moisture content of the samples was reached.

Spectral analysis

All ASD infrared spectra were mosaicked to produce artificial images, each representative for a plot in one of the three stages of the experiment. Each pixel within an image contains the spectral information collected from the corresponding sampling point in a plot. A spectral subset of bands was created for the 1800 – 2500 nm wavelength range to include the water absorption band around 1900 nm, the clay feature near 2200 nm and the K absorption feature near 2465 nm (Luleva et al., 2011). A continuum removal conversion was applied to all spectra to eliminate brightness differences and thus enhance colour difference while standardizing the shape of absorption features (Noomen et al., 2006). The absorption feature parameters- depth, position and area were computed for each pixel in IDL ENVI software, following van der Meer (2004). Each image pixel was then assigned the corresponding absorption parameter values for the water, clay and K absorption feature. The images were spatially interpolated using ordinary kriging with a spherical semivariogram model in ArcGIS 10 software. Validation of the spectrally obtained images was done by comparison with laboratory determined K concentrations in the collected water and soil samples, as well as digitized images of the flow patterns.

A spectral library was built from spectra collected during the controlled moisture experiment. Absorption band depth was calculated in IDL ENVI software following van der Meer (2004). The absorption depths of the water (near 1900 nm), clay (near 2200 nm) and K (near 2465 nm) absorption bands were plotted to determine the relation and coefficient of determination between moisture content, clay content and K content. The Normalized Soil Moisture Index (NSMI) was calculated in order to minimize the influence of varying soil texture and albedo (Haubrock et al., 2008). The same procedure was applied to the images corresponding to each experimental field plot.

The parameters derived from the spectra in the artificial images were subsequently analysed against the laboratory moisture tests to estimate the coefficient of determination (R^2) between the water, clay and K absorption bands.

Site description

The experiment was done in an agricultural field in South Limburg region, The Netherlands. This region is part of the European Loess belt which covers parts of England, Northwest France, Belgium, The Netherlands, Germany, Poland and Russia (Kwaad et al., 2006). Typical landforms include dry valleys, incised roads and manmade cultivation terraces. The soils belong to Typic Hapludalf soil type (Soil Taxonomy) or Albic Luvisol³) and were developed on the Loess during the Holocene period. These soils are highly vulnerable to soil erosion and runoff due to their low structural stability. Top soils contain up to 60% silt, while sub soils are stony and dry due to underlying gravel of palaeo river terraces deposited by the river Meuse. The slope varies from 2 to 12% (de Bakker, 1979). The annual precipitation is distributed throughout the whole year with high-intensity rainfall restricted between April and October. The average rainfall is 60mm per month, with maximum reaching 1-2 mm/min (Kwaad et al., 2006). Erosion is enhanced by a continuous change in land cover and decrease of grassland in favour of arable land (Boardman et al., 1994). The area is mainly used for crop production, therefore the soil is bare for the period outside the growing season (Winteraeken & Spaan, 2010).

Results

Laboratory analysis

Table 1 shows the characteristics of the soil found in each plot. These consist of the amount of fertilizer applied, initial soil moisture temperature values, water fraction per volume (WFV), total salt content, texture characteristics and bulk density per plot. The

Table 1. Field conditions in the experimental plots, obtained by geochemical analysis of soil samples obtained from each plot

Plot	Reference K		Added K ₂ O	Initial moisture characteristics			Texture %			Bulk density (g/cm ³)
	0-2cm (mg/g)	15-20 cm (mg/g)		0-2cm (mg/g)	Temperature (C)	WFV	Total salt (s/m)	Sand	Silt	
A	2.61	0.72	0.6	14.9	0.34	0.29	31	56	13	1.32
B	2.93	0.87	2.48	15.1	0.34	0.35	30	58	12	1.29
C	2.60	0.57	0	15.7	0.34	0.28	29	53	18	1.32

*WFV- water fraction per volume

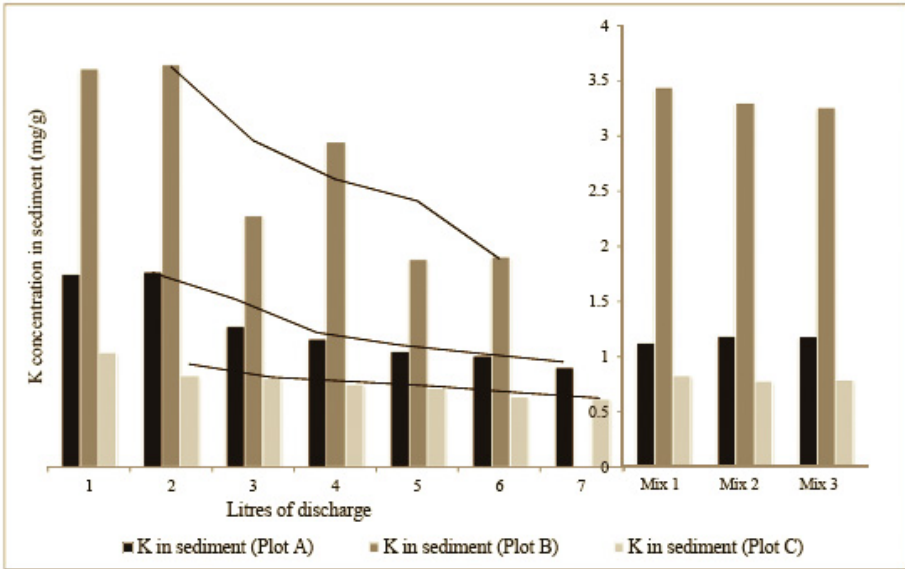


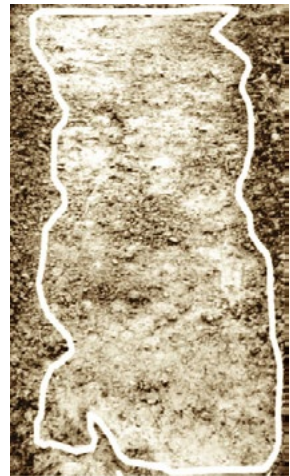
Fig. 2. Bar chart showing a decrease in K concentration measured in sediment per litre of discharge for plots A, B and C



A)



B)



C)

Fig. 3. Schematic outline of each plot with the area inside the white polygon that was covered by flowing water: the area outside the polygon remained dry

table shows that, in all plots, the K concentration at 15 cm depth is lower than at the surface. Bulk density varies with 0.03 g/cm^3 between the plots. Texture characteristics indicate that these soils have typical characteristics of silt loam derived from loess with silt content 53- 58% and maximum clay content of 18%.

Fig. 2 shows the change in K concentration per litre of discharge during the flow experiment. The concentration of K in the collected sediment collected decreases indicating removal of fertilizer.

Fig. 3 shows the area of each plot covered by water flow after the experiment was completed. It can be noted that parts of plots A and B were not affected by runoff water.

Spectral analysis

Fig. 4 shows the change in K absorption feature depth (near 2465 nm) for each plot at each stage of the experiment. It can be observed that for most pixels, depth of absorption features increases with addition of fertilizer. After water flow, K absorption deepens further for all plots.

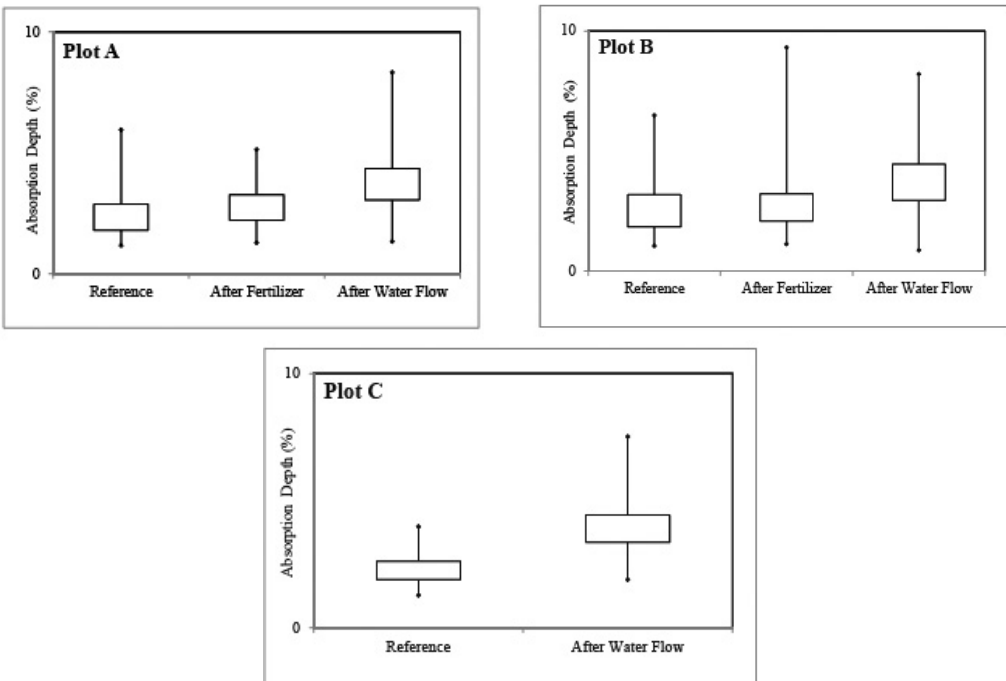


Fig. 4. Change in K absorption feature depth, for plots A, B and C in for each stage of the experiment

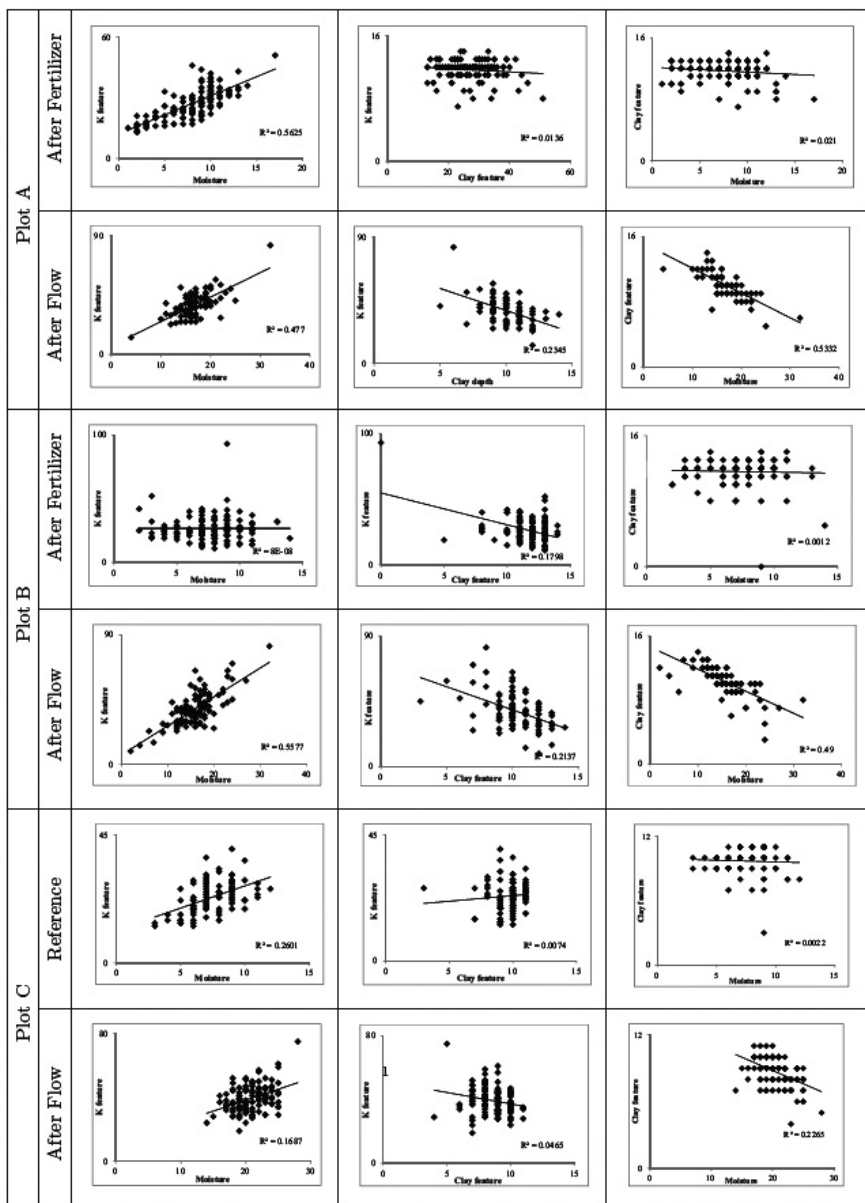


Fig. 5. Relationships between band depth near 2465 nm (K feature), band depth near 2200nm (Clay feature) and NSMI values (soil moisture) expressed using coefficient of determination (R^2)

Fig. 6. Spatial representation of K absorption feature depth near 2465 nm, NSMI and clay absorption feature depth near 2200 nm for plot A. This plot was treated with 0.6 mg/g of fertilizer. Each image comprises 108 sampling points collected after each stage of the field experiment (before treatment, after addition of fertilizer, and after water flow)
 “available in color online”

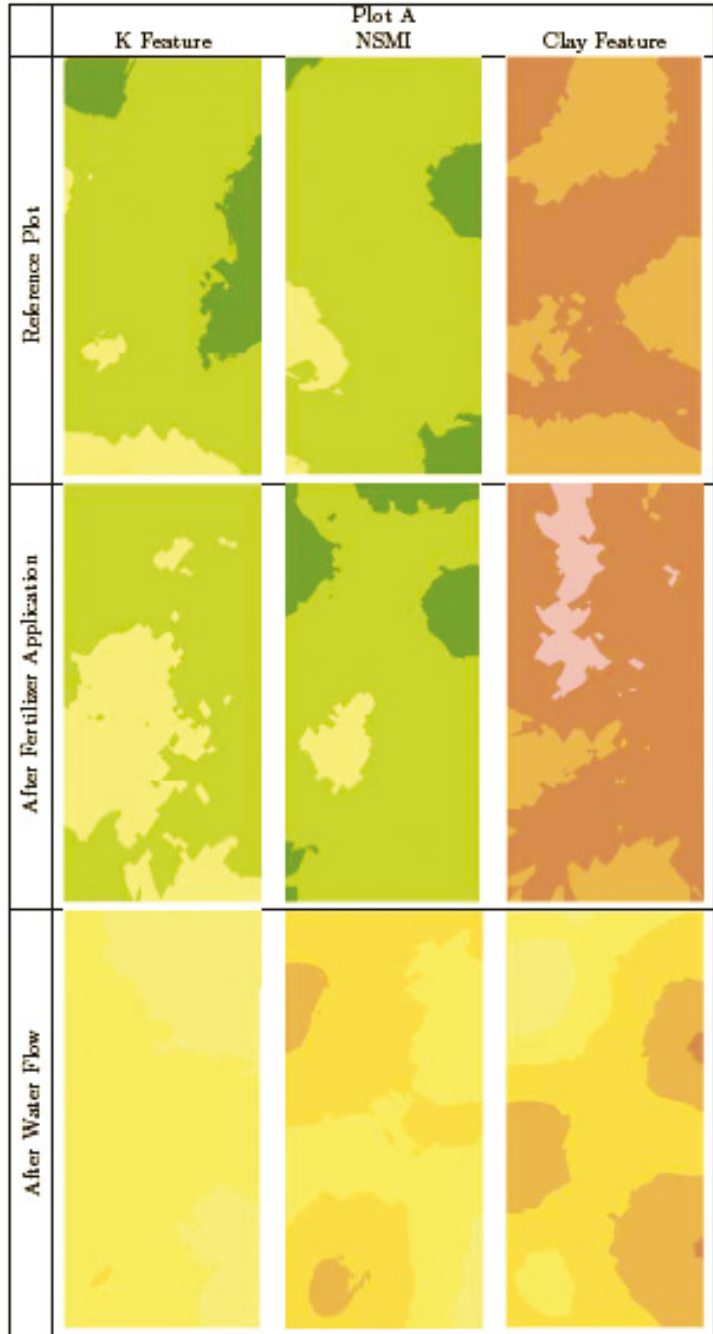
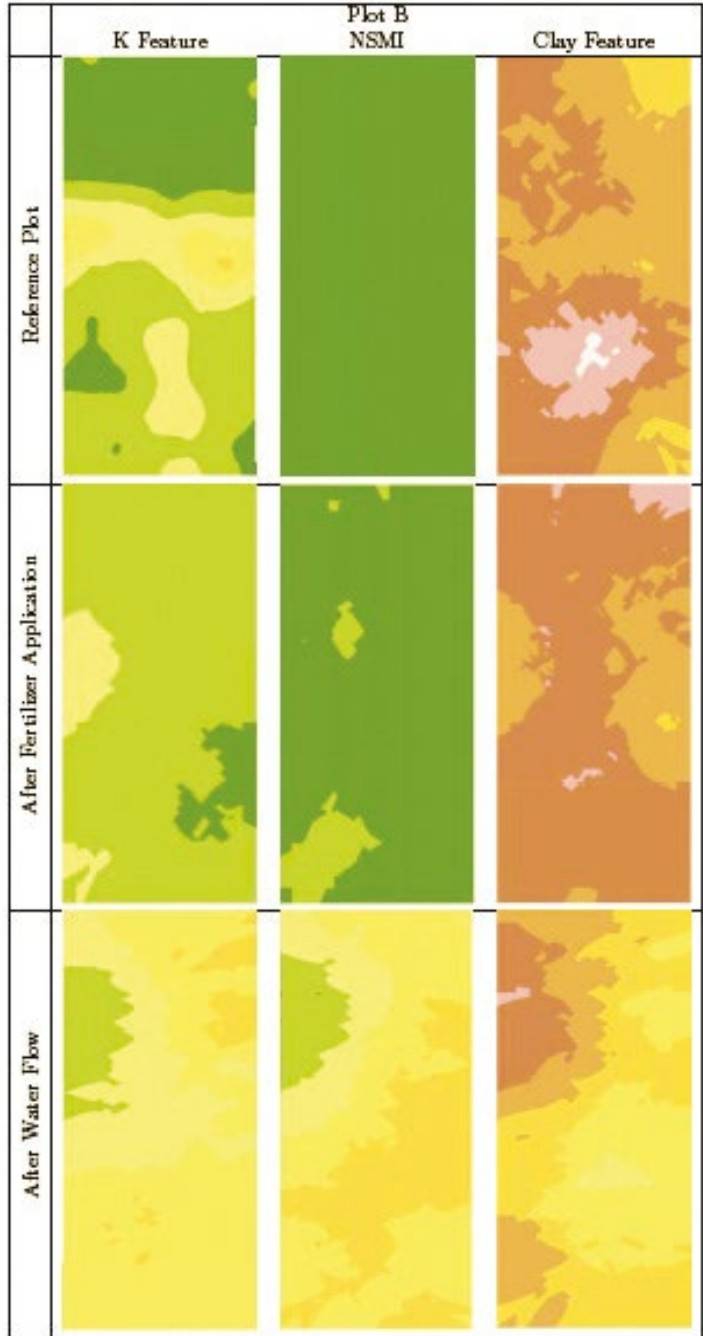


Fig. 7. Spatial representation of K absorption feature depth near 2465 nm, NSMI and clay absorption feature depth near 2200nm for plot B. This plot was treated with 2.4 mg/g of added fertilizer. Each image comprises 108 sampling points collected after each stage of the field experiment (before treatment, after addition of fertilizer, and after water flow) “available in color online”



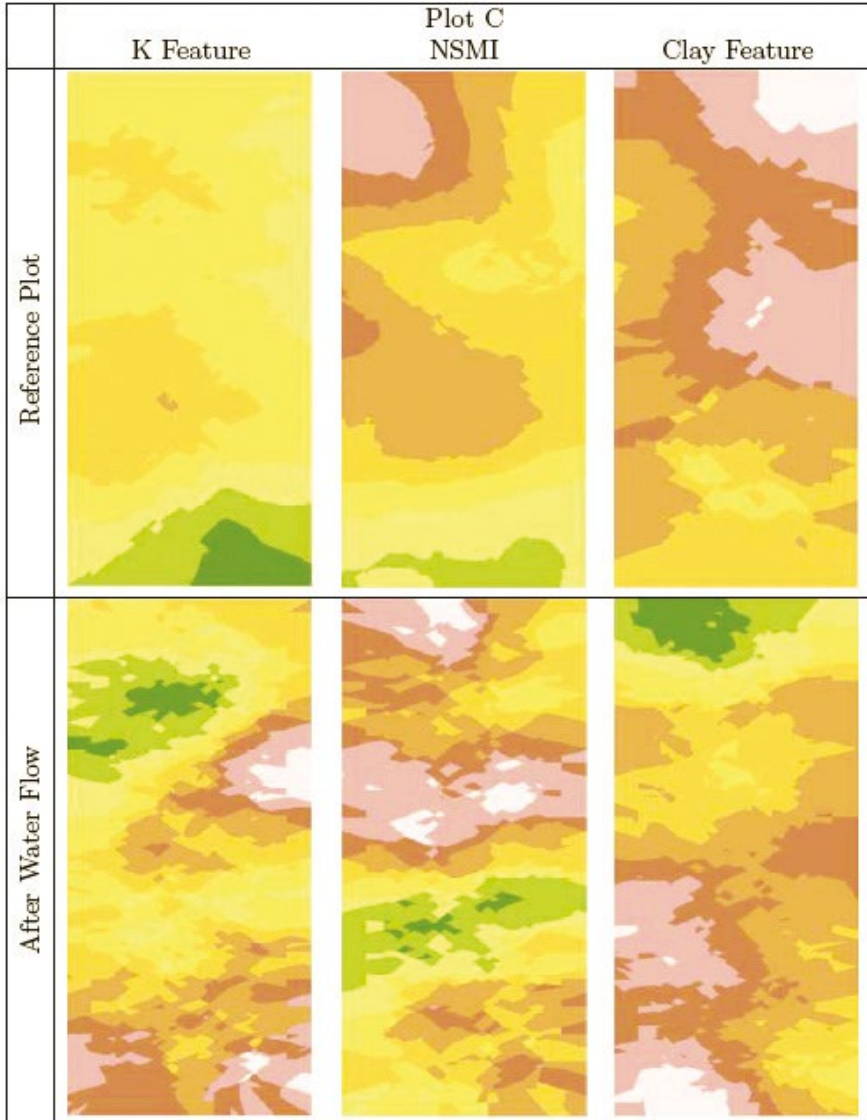


Fig. 8. Spatial representation of K absorption feature depth near 2465 nm, NSMI and clay absorption feature depth near 2200nm for plot C. This plot had no added fertilizer. Each image comprises 108 sampling points collected from the untreated plot and after water flow “available in color online”

Fig. 5 shows relationships between the NSMI index (soil moisture), clay absorption bands at 2200 nm and K absorption bands at 2465 nm. For all plots, after application of fertilizer, the values for R^2 indicate that the influence of moisture on K absorption is higher than this of clay. After water flow, however, R^2 values between clay and moisture, as well as clay and K feature increase.

Figs 6-8 show the results of absorption feature analysis. The natural variation in K can be observed from Figs 6-8 (top row) for each plot. The range of K absorption band depth is 1.3 - 8.3% for plot A, 1.3-8.5% for plot B, and 3.2-4.5 % for plot C. In all images, NSMI is highest after water flow. The images showing clay absorption band depth show a decreased absorption after water flow (Figs 6-8, right column).

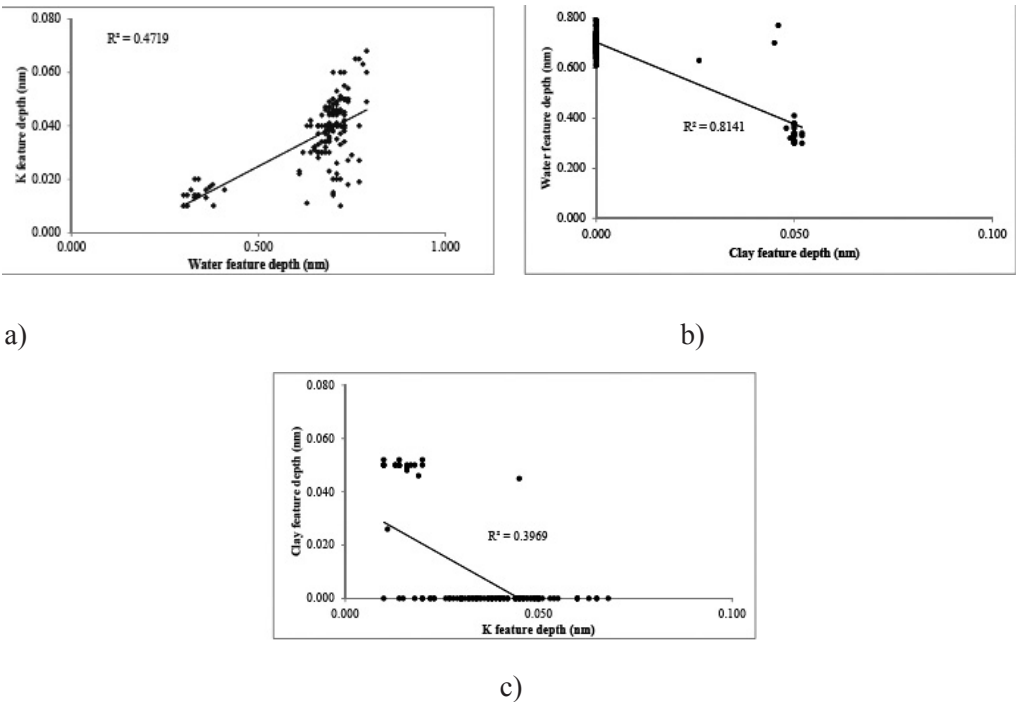


Fig. 9. Statistical relationships between depth of water absorption band (1900 nm), clay absorption band (2200 nm) and K absorption band (2465 nm) derived from laboratory spectra measured during a controlled moisture experiment; a) Moisture content vs. K feature depth; b) Moisture content vs Clay feature depth; c) Clay feature depth vs. K feature depth

Moisture test

Fig. 9 shows relationships between the absorption features of water, clay and potassium at 1900, 2200 and 2465 nm respectively. It can be observed that the feature at 2200nm, which is associated with clay content, becomes deeper as the soil dries. Values for coefficient of determination (R^2) of 0.47 and 0.40 between laboratory derived parameters (Fig. 9a and c) indicate that the influence of moisture and clay do not correspond to observations made during the field experiment. As seen in Fig. 5, the R^2 values the field are higher for all plots, showing stronger influence of moisture and clay on K absorption.

Discussion

Potassium fertilizer mobility

K adsorbs onto the surface of soil particles latest 10 minutes after application of fertilizer (Wang & Huang 2001). Once attached, K remains immobile (Garrett, 1996) unless displaced by water or taken up by plants (Jalali & Rowell, 2009). Soil particles are considered displaced if measured K concentrations are lower than what has been applied in the form of a fertilizer, or are similar to the concentration prior to application of fertilizer.

The K concentration in the mixed runoff sediment samples was 12 mg/g, which is 0.6 mg/g higher than the amount of K that was added with the fertilizer (0.6 and 2.4 mg/g for plot A and B respectively). This might be due to the release of slowly available K under the influence of water flow. Alternatively, it may so result from K fertilizer that had been applied by farmers before the experiment, as the experiment took place in an agricultural field. Unknown concentrations of K in the water that was used for the experiment could also add to these amounts. Soil texture is not considered to have an influence, since the texture analysis of the soil material indicates a comparable sand-silt-clay content of all plots (Table 1).

Change in absorption feature depth in relation to K concentrations

Figs 6 - 8 show the change in surface soil moisture, K absorption band depth and clay absorption band depth for all plots and all stages of the experiment. With the addition of K, a change in depth of the feature near 2465 nm is observed. Although the fertilizer was applied evenly to the surface of all plots, a uniform distribution cannot be observed. This is likely to be a result of natural variation in the initial K concentration or application of fertilizer by farmers prior to the experiment.

After water flow, the K absorption feature appears deeper. From Fig. 3 (a and b) that show flow coverage, and Figs 6 and 7 showing change in absorption depth, it can be observed that the patches that were not covered by the water flow have the shallowest spectral absorption features. Variations within the plots can also be due to larger parti-

cles that travel shorter distances and might be deposited early (Morgan, 2005), before reaching the end of the plot.

The spatial representation of soil moisture and clay content, as presented by NSMI and clay absorption band depth, shows their influence on spectroscopic detection of K in soils. In all images, NSMI increased after each stage of the experiment (Figs 6-8). The depth of clay absorption feature decreased after water flow, which can be explained by the removal of fine clay particles by flowing water. Fig. 9 shows an R^2 of 0.81 in the relationship between the depths of absorption features near 1900 nm and 2200 nm. As the soil dries, the 2200 nm clay feature becomes deeper and more pronounced, which is also observed by Kariuki et al. (2004). The presence of moisture and clay influences the K absorption feature near 2465 nm with an R^2 of 0.47 and 0.39 respectively. These relationships established based on laboratory tests differ from what was observed in the field. For plot A (Fig. 5), the relationship between clay and K absorption feature depth has an R^2 of 0.53. This is also shown in plot B (Fig. 5), where, after water flow, the influence of moisture and clay increases with an increase of R^2 from 0.00 to 0.56 and 0.18 to 0.21, respectively. This indicates that the behavior of K when applied in the field is highly influenced by external factors, that could not be predicted on laboratory level.

Based on the work of Luleva et al. (2011) and Yitagesu et al. (2011), it was expected that clay content would influence the depth of absorption near 2465 nm. The experimental field was hence selected in the Loess derived soils, which only have a maximum of 18% clay (Jacobs & Mason, 2007). However, as stated by Jacobs & Mason (2007), clay content in Loess soils can be higher if post sedimentation or exposure of clay-rich B horizon has taken place. The concentration of K applied to the plots was insufficient to show a spectral signature given the high amounts of water and clay are presented.

A direct relationship between the K absorption band depth near 2465 nm and its distribution in the field could not be established. This would probably be possible if higher amounts of fertilizer would have been added (as done in Luleva et al., 2011). These amounts however exceed what is recommended for agricultural practices. Exploring absorption features associated with K in the thermal (mid) infrared could counterfeit the influence of moisture and clay. Imaging spectrometers that acquire spatial data simultaneously could limit the noise that was now introduced while measuring individual points.

Potential use of potassium as a tracer for soil erosion

In all soil erosion studies using chemical particle tracers, the even distribution of the chemical has been assumed (Chappell, 1999). For L, the natural variation of the element due to parent material or crop residue, as well as previously applied fertilizer, presents a limitation. This could, however, be overcome by collecting and analysing soil spectra prior to fertilization.

Knowing the concentration of K prior to fertilizer application is crucial for using the element as a tracer. Compared to Cs, however, potassium (K) is spectrally active, and the absorption feature near 2465 nm allows rapid detection of its abundance in the environment prior to additional application of the element. Furthermore, this provides an opportunity to collect measurements before each stage of the field experiment. This helps determining the natural distribution of the element or previously applied quantities of fertilizer, as well as testing the method and distribution of added K before the flow experiment.

A factor that should be considered when using K as a tracer is its behaviour when introduced to the environment. While radioactive elements are considered to move only due to erosion, when attached to soil particles, K can be moved due to uptake by plants or by leaching into the subsurface. To prevent vegetation uptake and to allow collection of soil spectra using hyper-spectral imagers, measurements are limited to the time between fertilizer application and crop growth. In addition, clay and moisture content restrict the applicability of the method at concentrations of applied fertilizer lower than 2.48 mg/g soil, as presented in this study.

Conclusions

In this paper, we discussed the use of infrared spectroscopy for detecting changes in K concentrations in soils. Potassium (K) fertilizer for commercial use was applied in various concentrations to three experimental plots on silt loam soils. A flow experiment was conducted, and spectral measurements were collected to determine change in K before application of fertilizer, after application of fertilizer and after water flow. Laboratory and spectral analyses were performed to determine the change in absorption characteristics associated with K.

A relative change in abundance of K could be observed in the field using the spectral absorption feature near 2465 nm. The amount of K removed with water flow corresponds to concentrations of K found in the sediment of the runoff water, although background concentrations from either naturally occurring K or previously applied fertilizer had increased the amount of K. Change in the 2465 nm absorption feature depth does not seem to correspond to the controlled addition and removal of K. This is likely to be a result of external influences such as moisture and clay content.

Although previous studies indicate the suitability of the method at laboratory level (Luleva et al., 2011), in the field, the absorption feature near 2465 nm, associated with K, is highly influenced by moisture and clay content, at concentrations of K typically applied to agricultural fields.

If further work is intended, the method can only be applied successfully using quantities of fertilizer higher than 2.48 mg/g, or on soils with lower than 18 % clay content.

Establishing K as a particle tracer can provide an opportunity for increase in size of study area and density of sampling points. This however could be possible only give that the limitations, identified in the current study, can be overcome at field level.

Acknowledgements

The authors thank Mr. Boudewijn de Smeth and Mr. Henk Wilbrink (Faculty of Geo-information Science and Earth Observation (ITC), University of Twente) for their input in the laboratory experiments.

NOTES

1. http://scenarios.ew.eea.europa.eu/reports/fo1949029/fo1040583/Agriculture_final_report.pdf
2. http://www.isric.org/isric/webdocs/docs/ISRIC_TechPap09_2002.pdf?q=Isric/Webdocs/Docs/ISRIC_TechPap09_2002.pdf[http://www.isric.org/isric/webdocs/docs/ISRIC_TechPap09_2002.pdf](http://www.isric.org/isric/webdocs/docs/ISRIC_TechPap09_2002.pdf?q=Isric/Webdocs/Docs/ISRIC_TechPap09_2002.pdf)
3. <ftp://ftp.fao.org/agl/agll/docs/wsrr103e.pdf>

REFERENCES

- Alatorre, L.C. & Beguería, S. (2009). Identification of eroded areas using remote sensing in a badlands landscape on marls in the central Spanish Pyrenees. *CATENA*, 76, 182-190.
- Andrello, A.C. & Appoloni, C.R. (2004). Spatial variability and cesium-137 inventories in native forest. *Brazilian J. Physics*, 34, 800-803.
- Askegaard, M. & Eriksen, J. (2000). Potassium retention and leaching in an organic crop rotation on loamy sand as affected by contrasting potassium budgets. *Soil Use & Management*, 16, 200-205.
- Boardman, J. (2006). Soil erosion science: reflections on the limitations of current approaches. *CATENA*, 68, 73-86.
- Boardman, J., Ligneau, L., de Roo, A. & Vandaele, K. (1994). Flooding of property by runoff from agricultural land in northwestern Europe. *Geomorphology*, 10, 183-196.
- Campbell, B.L., Loughran, R.J. & Elliott, G.L. (1982). Caesium-137 as an indicator of geomorphic processes in a drainage basin system. *Australian Geographical Studies*, 20, 49-64.
- Chappell, A. (1999). The limitations of using 137Cs for estimating soil redistribution in semi-arid environments. *Geomorphology*, 29, 135-152.
- De Bakker, H. (1979). *Major soils and soil regions in the Netherlands*. Hague: W. Junk.
- De Graffenried, Jr, J.B. & Shepherd, K.D. (2009). Rapid erosion modeling in a Western Kenya watershed using visible near infrared reflectance, classification tree analysis and 137Cesium. *Geoderma*, 154, 93-100.
- Estrany, J., Garcia, C. & Walling, D.E. (2010). An investigation of soil erosion and redistribution in a Mediterranean lowland agricultural catchment using caesium-137. *Intern. J. Sediment Research*, 25, 1-16.
- Garrett, D.E. (1996). *Potash: deposits, processing, properties and uses*. London: Chapman & Hall.

- Haubrock, S.-N., Chabrillat, S., Lemmnitz, C. & Kaufmann, H. (2008). Surface soil moisture quantification models from reflectance data under field conditions. *Intern. J. Remote Sensing*, 29, 3 - 29.
- Hengl, T., Rossiter, D.G. & Stein, A. (2003). Soil sampling strategies for spatial prediction by correlation with auxiliary maps. *Soil Research*, 41, 1403-1422.
- Jacobs, M. & Mason, J. (2007). Late quaternary climate change, loess sedimentation, and soil profile development in the central Great Plains: a pedosedimentary model. *Geological Soc. Am. Bulletin*, 119, 462-475.
- Jalali, M. & Rowell, D.L. (2003). The role of calcite and gypsum in the leaching of potassium in sandy soils. *Experimental Agriculture*, 39, 379-394.
- Jalali, M. & Rowell, D.L. (2009). Potassium leaching in undisturbed soil cores following surface applications of gypsum. *Environmental Geology*, 57, 41-48.
- Jetten, V., Govers, G. & Hessel, R. (2003). Erosion models: quality of spatial predictions. *Hydrological Processes*, 17, 887-900.
- Kariuki, P.C., Woldai, T. & Van Der Meer, F. (2004). Effectiveness of spectroscopy in identification of swelling indicator clay minerals. *Intern. J. Remote Sensing*, 25, 455-469.
- Kwaad, F.J.P.M., de Roo, A.P.J. & Jetten, V.G. (2006). The Netherlands (pp. 477-487). In: Boardman, J. & Poesen, J. (Eds.). *Soil Erosion in Europe*. New York: Wiley.
- Luleva, M.I., van der Werff, H., Jetten, V. & van der Meer, F. (2011). Can infrared spectroscopy be used to measure change in potassium nitrate concentration as a proxy for soil particle movement? *Sensors*, 11, 4188-4206.
- Meusburger, K., Konz, N., Schaub, M. & Alewell, C. (2010). Soil erosion modeled with USLE and PESERA using QuickBird derived vegetation parameters in an alpine catchment. *Intern. J. Applied Earth Observation & Geoinformation*, 12, 208-215.
- Morgan, R.P.C. (2005). *Soil erosion and conservation*. Malden: Blackwell.
- Noomen, M.F., Skidmore, A.K., van der Meer, F.D. & Prins, H.H.T. (2006). Continuum removed band depth analysis for detecting the effects of natural gas, methane and ethane on maize reflectance. *Remote Sensing of Environment*, 105, 262-270.
- Onda, Y., Kato, H., Tanaka, Y., Tsujimura, M., Davaa, G. & Oyunbaatar, D. (2007). Analysis of runoff generation and soil erosion processes by using environmental radionuclides in semiarid areas of Mongolia. *J. Hydrology*, 333, 124-132.
- Parsons, A.J. & Foster, I.D.L. (2011). What can we learn about soil erosion from the use of ¹³⁷Cs? *Earth-Science Rev.*, 108, 101-113.
- Porto, P., Walling, D.E. & Ferro, V. (2001). Validating the use of caesium-137 measurements to estimate soil erosion rates in a small drainage basin in Calabria, Southern Italy. *J. Hydrology*, 248, 93-108.
- Relman, A.S. (1956). The Physiological behavior of rubidium and cesium in relation to that of potassium. *Yale J. Biology & Medicine*, 29, 248-262.
- Rodway-Dyer, S.J. & Walling, D.E. (2010). The use of ¹³⁷Cs to establish longer-term soil erosion rates on footpaths in the UK. *J. Environ. Management*, 91, 1952-1962.
- Saç, M., Uğur, A., Yener, G. & Özden, B. (2008). Estimates of soil erosion using cesium-137 tracer models. *Environmental Monitoring & Assessment*, 136, 461-467.

- Van der Meer, F. (2004). Analysis of spectral absorption features in hyperspectral imagery. *Intern. J. Applied Earth Observation & Geoinformation*, 5, 55-68.
- Vrieling, A. (2006). Satellite remote sensing for water erosion assessment: a review. *CATENA*, 65, 2-18.
- Walling, D.E. & Quine, T.A. (1990). Calibration of caesium-137 measurements to provide quantitative erosion rate data. *Land Degradation & Development*, 2, 161-175.
- Wang, F.L. & Huang, P.M. (2001). Effects of organic matter on the rate of potassium adsorption by soils. *Canadian J. Soil Science*, 81, 325-330.
- Winteraeken, H.J. & Spaan, W.P. (2010). A new approach to soil erosion and runoff in south Limburg—The Netherlands. *Land Degradation & Development*, 21, 346-352.
- Witzke H.P., Britz, W. & Zintl, A. (2004). Outlooks on selected agriculture variables for the 2005 State of the Environment and the Outlook Report, EuroCARE Bonn, Final Report, EEA/RNC/03/016.
- Xiaojun, N., Xiaodan, W., Suzhen, L., Shixian, G. & Haijun, L. (2010). ¹³⁷Cs tracing dynamics of soil erosion, organic carbon and nitrogen in sloping farmland converted from original grassland in Tibetan plateau. *Applied Radiation & Isotopes*, 68, 1650-1655.
- Yitagesu, F.A., van der Meer, F., van der Werff, H. & Hecker, C. (2011). Spectral characteristics of clay minerals in the 2.5–14 μm wavelength region. *Applied Clay Science*, 53, 581-591.
- Zhang, X.C., Friedrich, J.M., Nearing, M.A. & Norton, L.D. (2001). Potential use of rare earth oxides as tracers for soil erosion and aggregation studies. *Soil Sci. Soc. Am. J.*, 65, 1508-1515.

Ms. Mila Ivanova Luleva (corresponding author)

✉ E-Mail: lule14713@itc.nl

Dr. Harald van der Werff,

✉ E-Mail: vdwerff@itc.nl

Dr. Freek van der Meer,

✉ E-Mail: vdmeer@itc.nl

Dr. Victor Jetten,

✉ E-Mail: jetten@itc.nl

Faculty of Geo-Information Science and Earth Observation (ITC),
University of Twente,
Hengelosestraat 99, Enschede, The Netherlands